HHS Public Access

Author manuscript

Neurosci Lett. Author manuscript; available in PMC 2022 April 17.

Published in final edited form as:

Neurosci Lett. 2021 April 17; 750: 135799. doi:10.1016/j.neulet.2021.135799.

Learning and Synaptic Plasticity in 3D Bioengineered Neural Tissues

Nicolas Rouleau[1,2,3], **Dana M. Cairns**[1,2,3], **William Rusk**[1], **Michael Levin**[2,3,4], **David L. Kaplan**[1,2,3]

[1]Department of Biomedical Engineering, Tufts University

[2]The Allen Discovery Center, Tufts University

[3]Initiative for Neural Science, Disease, and Engineering (INSciDE), Tufts University

[4]Department of Biology, Tufts University

Abstract

Though neuroscientists have historically relied upon measurement of established nervous systems, contemporary advances in bioengineering have made it possible to design and build artificial neural tissues with which to investigate normative and diseased states[1–5]; however, their potential to display features of learning and memory remains unexplored. Here, we demonstrate response patterns characteristic of habituation, a form of non-associative learning, in 3D bioengineered neural tissues exposed to repetitive injections of current to elicit evoked-potentials (EPs). A return of the evoked response following rest indicated learning was transient and partially reversible. Applying patterned current as massed or distributed pulse trains induced differential expression of immediate early genes (IEG) that are known to facilitate synaptic plasticity and participate in memory formation[6,7]. Our findings represent the first demonstration of a learning response in a bioengineered neural tissue *in vitro*.

Keywords

learning; bioengineering; evoked-potentials; synaptic plasticity; habituation

Corresponding author: Dr. David L. Kaplan (DLK), David.kaplan@tufts.edu.

Author Contributions

NR, and DLK conceived of the project and designed experiments. NR, DMC, and WR performed experiments and collected data. NR and DMC analyzed data and interpreted results. NR and DLK wrote the manuscript. ML and DLK provided resources, laboratory space, and secured funding for the project.

Competing Interests

The authors declare no conflicts of interest, monetary or otherwise.

Introduction

Learning, the process by which a system acquires or modifies information[8], is an intrinsically adaptive biological strategy. Once dedicated to an animal's memory, the utility of learned responses parallel those conferred to the species through natural selection by facilitating the avoidance of noxious events[9,10], the pursuit of rewards[11,12], and ultimately, self-propagation. Non-associative learning represents a rudimentary operation that has been observed ubiquitously in nature from primates[13,14] to protozoa[15,16]. It is operationally defined as any change to the parameters of a response upon repetitive stimulation[17]. That is, when continually stimulated, most organisms learn to either suppress (habituate) or enhance (sensitize) their outputs contingent upon a history of inputs. Until recently, the study of learning was restricted to the observation and manipulation of naturally-derived organisms and their established nervous systems; however, recent advances in neural tissue engineering have made it possible to build minimal, synthetic tissue constructs with which to explore the structure-function degeneracy of cognitive processes such as learning and memory.

We therefore hypothesized that synthetic neural tissues, designed and fabricated in the laboratory, could exhibit stimulus-response patterns similar to those observed in animals[18,19] and slice preparations[20]. As previously reported, our bioengineered tissue model is composed of a three-dimensional (3D) silk-based scaffold seeded with embryonic rat neurons and glia[21]. Unlike classical cortical histoarchitecture which reflects a predictable laminar morphology, the anatomy of our neural tissue constructs can be customized according to desired specifications. Without an imposed design, neurons self-assemble into dense, haphazard networks within the scaffolds. The tissues display robust electrophysiological activity[22] and secrete expected biochemical factors[23]; however, it remains unclear whether they are capable of complex functional responses. The goal of the present work was to demonstrate reversible learning responses and paired synaptic plasticity in an artificial, bioengineered neural tissue.

Methods

Bioengineered neural tissues

Bioengineered 3D cortical tissues (Figure 1) were assembled, following our established protocol[24]. Briefly, the brains of embryonic rat pups (E18, Sprague-Dawley, Charles River) were harvested and their cortices were resected. Following trypsin-digestion and re-suspension of neurons and glia, silk fibroin (6% w/v) scaffolds (6 mm diameter, 2 mm height, 2 mm central window) were seeded with 10^6 cells suspended in a 100 μL aliquot of media, which was composed of Gibco Neurobasal medium (Thermo Fisher), 1% v/v L-alanine-L-glutamine dipeptide (GlutaMAX) supplement (Thermo Fisher), 2% v/v B27 supplement (Thermo Fisher), and 1% v/v penicillin-streptomycin (Corning). Attachment proceeded undisturbed until 24-hours post-seeding, whereupon samples were embedded in collagen type-I (rat) hydrogels (3 mg/mL) that were pH-adjusted to 7.4 using NaOH. Samples were maintained in 1 mL/scaffold of media in 24-well plates for 2 weeks to promote growth, connectivity, and maturation before testing.

Patch-Clamp Recordings

Patch-clamp experiments (Figure S1A) in the whole-cell configuration were carried out in the I/0 configuration after 14 days of 2D culture at T=37±1°C. Neurons were superfused with an external solution containing (mM): 129 NaCl, 1.25 NaH_2PO_4, 1.8 $MgSO_4$, 1.6 $CaCl_2$, 3 KCl, 10 Na-HEPES, 35 glucose, pH 7.4. The pipette resistance was 5–8 MΩ when filled with an intracellular-like (mM): 120 K-gluconate, 15 KCl, 2 $MgCl_2$, 0.2 EGTA, 20 phosphocreatine, 2 ATP-disodium, 0.2 GTP-disodium, 0.1 leupeptin, 10 HEPES-KOH, pH 7.2. To investigate the single cell response to a habituation protocol, neurons were held at −70 mV and two 20s-long electric stimulations (20 s inter-stimulation interval) was delivered as a pulse train (frequency:1Hz; stimulus magnitude: 80 pA; stimulus duration: 300 ms duration). Neither series resistance compensation, liquid junction potential, or leak correction were applied.

Local Field Potentials (LFPs) of 3D Cultures

Electrophysiological activity in of 3D cultures was measured by local field potentials (LFPs) collected along the surface of each tissue sample. Before initiating the habituation protocol (described elsewhere), samples were transferred to 35 mm plastic petri dishes (Corning) with 2mL of the extracellular solution (described elsewhere). To approximate physiological conditions, samples were maintained at 37°C (WP-16 Warmed Platform, Warner Instruments). Potential differences (mV) were measured between an Ag-AgCl reference electrode placed at the periphery of the petri dish and a glass pipette (80–140 MΩ) which was inserted into the scaffold region of the tissue sample. Signals were relayed to a digital amplifier and then to an Axon Instruments analog-to-digital converter. Traces were recorded in Clampex 10.7 (Axon Instruments) with a sampling rate of 2500 Hz and exported to Clampfit 10.7 (Axon Instruments) to perform an analysis of evoked-potentials (EPs). To validate the LFP collection procedure, we measured spontaneous activity in scaffolds containing cells (+Cells) and compared them to scaffolds containing no cells (−Cells) (Figure S1B).

Habituation Protocol

To generate current, we coupled an A310 Accupulser to an A365 Stimulus Isolator (World Precision Instruments). Bipolar electrodes delivered current to the surface of the scaffolds. The LFP probe from which voltage (mV) was recorded was positioned directly between the prongs of the bipolar electrode. The applied current pulse (1 ms width, square wave) was set to 5000 μA, 500 μA, or 50 μA (intensity variable) and was delivered as a unipolar signal, travelling across the tissue surface and through the recording region. The signal frequency was either 0.5, 1, or 2 Hz. The number of stimulations was held constant across conditions such that increased frequencies resulted in less total stimulation time relative to lower frequencies. Tetrodotoxin (TTX, 10 μM) was used to block voltage-gated sodium channels and suppress action potential generation associated with the applied current. Stimulating samples while blocked by TTX at the end of each trial served as a means to remove variance generated by the applied current, unmasking the contribution of the underlying biological signal[22].

The paradigm (Figure 2B) proceeded as follows: (1) 1 minute of baseline recording, (2) 30 stimulations, (3) 30 seconds of rest with baseline recording, (4) 30 stimulations, (5) 30 seconds of baseline recordings, (6) an injection of TTX, (7) 1 minute of baseline recording and TTX perfusion, and (8) 30 stimulations while blocked by TTX. To extract EPs, spikes generated by applied current were isolated using the threshold search function in Clampfit 10.7, specifying a 0.4 mV threshold, extracting a trace with pre- and post-trigger lengths of 1.5 and 12.5 ms respectively. In some cases, spike detection was not achieved, and individual stimulations were excluded from the analysis – therefore some trials involved less than 30 stimulation events. To reduce trial-to-trial variability, only the first 15 EPs were analyzed. Because a plateau was achieved after < 5 stimulations, 15 EPs were more than sufficient. Once extracted, the TTX-blocked signals were used to generate an averaged waveform characteristic of the trial-specific current application and subtracted from the stimulation phases to reveal EPs. To validate the method, we stimulated both +Cells and −Cells scaffolds to compare averaged raw EP amplitudes (Figure S1C).

Analysis of Evoked Potential Data

A 5 ms window following the 1 ms stimulation width was extracted to detect maximum peak amplitude of the EPs for each stimulation trace. mV values were then exported to IBM SPSSv20 and z-transformed (number of standard deviations from the mean; do not reflect absolute mV magnitude) within trials to generate normalized time-series' reflective of the successive amplitudes of the evoked potentials for a given trial (Figure S1D). These data were then re-scaled from 0 to 1 using the min-max normalization method to eliminate negative z-score values while preserving their distribution (Figure S1E, F). To quantify habituation, the average re-scaled z-score associated with the last 3 stimulations was divided by the average re-scaled z-score associated with the first 2 stimulations to generate a habituation quotient (HQ)[30,25] where a value of 1 represented non-habituation. As we predicted, repetitive stimulation generated a directional response (i.e., decreased EP magnitude over time), thus, it was sensible to use one-tailed hypothesis testing with an $\alpha = 0.10$. The more conservative α-levels of 0.05 or 0.001 are also reported throughout the text.

Massed vs Distributed Training Paradigm

Supplemental to the main paradigm, supportive experiments were designed to demonstrate the role of stimulation pattern on synaptic plasticity. Samples were transferred to 35 mm plastic petri dishes containing warmed extracellular solution (LFPs were not measured). Pulses of current (1 Hz, 5000 μA) were injected into the samples with either a massed (M) or distributed (D) training schedule. In the case of both stimulation patterns, 60 pulses were delivered in total; however, the group receiving the distributed training was injected with current in trains of 20 pulses, each separated by 1 minute whereas the group receiving the massed training was injected with one block of 60 stimulations. The stimulation protocol was not modeled after typical LTP-inducing sequences that involve bursts of high frequency (~100Hz) pulses with inter-stimulus intervals on the order of tens or hundreds of milliseconds. Other samples were manipulated, exposed to the same extracellular solution, equipment, and temperature but never stimulated; because distributed and massed training occurred over longer and shorter periods respectively, two control conditions were generated: distributed control (CD) and massed control (CM) to accommodate time outside

of the incubator. After receiving 60 stimulations, samples were returned to their wells containing media and incubated for 1 hour to promote synaptic plasticity[26,27]. After 1 hour, samples were washed in phosphate buffered saline, placed in RNA lysis buffer, vortexed, and stored at −80°C until RT-PCR was performed.

Real-Time Quantitative RT-PCR Array

Total RNA was isolated from bioengineered 3D cortical tissues using the RNeasy Mini kit (Qiagen). Isolated RNA was quantified using Nanodrop (Thermofisher) before conversion to cDNA using iScript (BioRad) according to manufacturers' protocols. Quantitative RT-PCR was performed using SYBR green and the CFX96 Real-Time PCR Detection System (BioRad) in accordance with the Qiagen RT² Profiler™ PCR Array for markers of Rat Synaptic Plasticity (catalog #ARN-126Z). Expression values were normalized against the housekeeping gene ß2 microglobulin (B2M).

Results

Evaluation of the habituation response

Bioengineered neural tissues (Figure 1) were exposed to a non-associative learning paradigm mirroring established habituation protocols *in vivo*[18,19] and in *vitro*[20,28]. In brief, tissues were pulsed with weak current at fixed frequencies and schedules to elicit EPs as inferred by punctate increases in LFP measurements (Figure 2A). It was predicted that EPs would be diminished as a function of the repetitive stimulation protocol (Figure 2B). A repeated measures ANOVA revealed simple effects of time [$F(14,1260)=5.65$, $p<0.001$] (Figure 2C) and stimulus frequency [$F(2, 90)=7.26$, $p<0.001$] on peak normalized EPs with a marginal two-way interaction ($p=0.06$). No significant effect of amplitude was detected ($p>0.05$). Comparisons across stimulation events (time) revealed a decrement between the first event and every subsequent event ($p<0.05$ – $p<0.001$). Plotting mean differences between the first event and each subsequent event revealed a positive association ($r=0.60$), indicating a progressive decrement (Figure 2D). The result was consistent with the expected habituation profile. Post-hoc tests indicated that the 2 Hz condition was associated with greater overall peak normalized EPs relative to the 1 Hz ($p<0.05$) and 0.5Hz ($p<0.001$) conditions. While indicative of learning, further tests were required to explore the putative interaction between time and frequency in detail as well as the reversibility of the learned response.

All combinations of conditions are presented in Figure 2E. Selecting for each frequency independent of amplitude, paired t-tests were performed to compare the first stimulation event with every subsequent event. Peak normalized EPs decreased from the first to the second stimulation event for both 0.5 Hz ($p<0.01$) and 1 Hz ($p<0.001$) conditions; however, at least 2 events were required on average before a similar decrease could be observed for the 2 Hz condition. A stable decrement associated with the 1Hz condition was also observed where peak normalized EPs associated with each sequential event were significantly decreased relative to the first event. This was not the case for the 0.5 Hz and 2 Hz conditions ($p>0.05$). Together, these results indicated a general frequency-dependence of habituation, the initiation of the decrement, as well as its stability.

Quantification of the degree of habituation

To further quantify the learning response a habituation quotient (HQ) was computed[29,30]. A one-way ANOVA revealed an effect of frequency on HQ, $F(2,98)=2.39$, $p<0.10$. The 2 Hz condition displayed reduced HQ values relative to other conditions, indicative of habituation (Figure 3A). We then hypothesized that either the initial magnitude of the response or the net decrement was driving the observed difference due to frequency. An ANOVA identified an effect of frequency on the first 2 EPs [$F(2,98)=4.60$, $p=0.01$] but not for the last 3 EPs ($p>0.05$). The 2 Hz condition was associated with greater normalized peaks among the first 2 EPs relative to other frequency conditions ($p<0.005$). These results suggested the magnitude of the initial EPs relative to subsequent EPs was affected by frequency where more frequent stimuli generated a more extreme initial response relative to later responses.

Determining reversibility of the learned response

Next, we investigated whether the tissues displayed “spontaneous recovery” after a rest period following the initial stimulation phase[17]. When individual cells were subjected to a similar protocol (patch-clamp), we not only elicited a decrement in evoked action potentials, but we demonstrated that the response recovered after a 20 sec rest period (Figure S1A) To test for recovery in the 3D bioengineered samples, we selected all trials that displayed an extreme initial normalized EP ($z > 2$) indicative of the classic habituation curve ($n=21$). Of this subset, there were $n=5$, $n=12$, and $n=4$ trials associated with the 2 Hz, 1 Hz, and 0.5 Hz conditions respectively. Examined together, a partial recovery was evident with a paired t-test revealing a significantly increased normalized EP following the rest period $t(20)=4.20$, $p<0.001$ (Figure 3B). The impact of frequency became apparent when each group was examined in isolation (Figure 3C). The 0.5 Hz condition displayed a significantly increased EP following the rest period ($p<0.005$) with a full recovery relative to the first EP of the habituation phase ($p>0.05$). The 1 Hz condition displayed a similar increase ($p<0.005$) with a partial recovery relative to the first EP of the habituation phase ($p<0.05$). The 2 Hz condition, however, did not display any indication of spontaneous recovery. Considered together, these data indicated that learning was reversible in the bioengineered tissues.

Assessing synaptic plasticity

As has been known for over a century[31], the efficiency and stability of learned responses in behaving organisms are contingent upon the spatiotemporal distribution of stimulation events. That is, animals learn differently if engagement with stimuli are experienced continuously (i.e., massed) or spread over several discrete periods (i.e., distributed)[32]. Similarly, but distinct from the applied pattern presented here, the quintessential memory-encoding process long-term potentiation (LTP) is also quite sensitive to the distribution of stimulation events. Therefore, we asked whether the same principles would apply to our artificial neural constructs.

To assess synaptic plasticity, quantitative RT-PCR analysis of 3D tissue constructs revealed marked differences in gene expression as a function of the training pattern (Figure 4A,B). Distributed (D) training generated increased expression of genes that are known to govern synaptic plasticity relative to its equivalent control condition (CD). There were no significant differences between massed training (M) and equivalent controls (CM). Several genes

associated with the Early Growth Response (EGR) family of transcriptional factors emerged as significantly upregulated in tissues exposed to distributed training relative to other groups. We also examined several genes that suppress memory and learning (e.g., Ppp1ca) or those that were non-specific (e.g., Ppp1cc, Ppp3ca, Mapk1); however, no significant differences were observed between tissues exposed to distributed training and equivalent controls (Figure S2). These data suggested that bioengineered tissues can be induced to express the early molecular markers of memory formation.

Discussion

We observed a clear frequency-dependent (Figure 3A) and partially reversible (Figure 3B,C) habituation response which achieved an asymptote (Figure 2C). Some results were unexpected, including displays of variable EPs following the initial decrement (Figure 2E) and the absence of spontaneous recovery associated with the 2Hz condition (Figure 3C). The former result may indicate the heterogeneity of the tissues or variable placement of the electrodes relative to embedded networks. With regard to spontaneous recovery, the trend suggests that as frequency decreased, recovery was more likely (Figure 3C); however, the underlying mechanism is not apparent from the data. Perhaps the 2Hz condition produced a more long-lasting habituation response that exceeded the brief (30 sec) interval between the initial and secondary stimulation periods though conclusions cannot be draw as other intervals were not tested.

Results from the RT-PCR assay revealed an upregulation of immediate early genes (IEGs) including Fos, Jun, and Egr1–4 (Figure 4B). The EGR transcriptional factors (Figure 4C) are known to underly synaptic plasticity and long-term memory formation6,7. Like other IEGs, EGR family members are rapidly and transiently expressed in response to neuronal activation. LTP, electroconvulsive shock, and learning paradigms are known to increase Egr family expression[33–35]. The pulsed injections of current that we used to stimulate the bioengineered neural tissues are, however, distinct from those used in classic LTP, as explained previously. As expected the distributed current pattern successfully induced synaptic plasticity. The spontaneous recovery data presented in Figure 3B,C and the gene expression data indicate that cells did not die when injected with current; rather, responses were dependent upon the parameters of the applied stimuli. Egr1 and Egr3 are involved in the maintenance of LTP as well as long- and short-term memory respectively[7,36,37], whereas Egr2 is thought to facilitate memory consolidation[7]. Egr4, however, does not have any known role in memory, though it may be linked to intelligence[38]. While these results are interesting and supportive of the main hypothesis, a detailed exploration of mechanisms underlying the expressed response to distributed training was beyond the scope of the present work.

The bottom-up design, assembly, and experimental manipulation of bioengineered neural tissues is expected to reveal how complex functions can emerge from minimal parameters. Our previous work has focused on disease and injury[23,39]; however, the model's suitability as a platform to study normative processes such as learning is evident. In addition to the present work, our recent use of calcium signaling to reveal the sub-surface, network-like

dynamics of the model system[40] contributes to an ongoing effort toward the recapitulation of high-order functions such as problem-solving and decision-making *in vitro*.

Supplementary Material

Refer to Web version on PubMed Central for supplementary material.

Acknowledgements

The authors would like to acknowledge the helpful contributions of Dr. Mattia Bonzanni and Dr. Joshua D. Erndt-Marino for their helpful comments and lending their expertise. We thank the NIH (P41EB0270620, R01NS092847) and the Paul Allen Foundation (2171) for support of this work.

References

[1]. Nisbet DR, Crompton KE, Horne MK, Finkelstein DI, & Forsythe JS (2008). Neural tissue engineering of the CNS using hydrogels. Journal of Biomedical Materials Research Part B: Applied Biomaterials: An Official Journal of The Society for Biomaterials, The Japanese Society for Biomaterials, and The Australian Society for Biomaterials and the Korean Society for Biomaterials, 87(1), 251–263.

[2]. Phillips JB, Bunting SC, Hall SM, & Brown RA (2005). Neural tissue engineering: a self-organizing collagen guidance conduit. Tissue engineering, 11(9–10), 1611–1617. [PubMed: 16259614]

[3]. Stabenfeldt SE, García AJ, & LaPlaca MC (2006). Thermoreversible laminin-functionalized hydrogel for neural tissue engineering. Journal of Biomedical Materials Research Part A: An Official Journal of The Society for Biomaterials, The Japanese Society for Biomaterials, and The Australian Society for Biomaterials and the Korean Society for Biomaterials, 77(4), 718–725.

[4]. Subramanian A, Krishnan UM, & Sethuraman S (2009). Development of biomaterial scaffold for nerve tissue engineering: Biomaterial mediated neural regeneration. Journal of biomedical science, 16(1), 108. [PubMed: 19939265]

[5]. Wang A, Tang Z, Park IH, Zhu Y, Patel S, Daley GQ, & Li S (2011). Induced pluripotent stem cells for neural tissue engineering. Biomaterials, 32(22), 5023–5032. [PubMed: 21514663]

[6]. Beckmann AM, & Wilce PA (1997). Egr transcription factors in the nervous system. Neurochemistry international, 31(4), 477–510. [PubMed: 9307998]

[7]. Poirier R, Cheval H, Mailhes C, Garel S, Charnay P, Davis S, & Laroche S (2008). Distinct functions of egr gene family members in cognitive processes. Frontiers in neuroscience, 2, 2. [PubMed: 18982094]

[8]. De Houwer J, Barnes-Holmes D, & Moors A (2013). What is learning? On the nature and merits of a functional definition of learning. Psychonomic bulletin & review, 20(4), 631–642. [PubMed: 23359420]

[9]. Schild LC, & Glauser DA (2013). Dynamic switching between escape and avoidance regimes reduces Caenorhabditis elegans exposure to noxious heat. Nature communications, 4(1), 1–11.

[10]. Vlaeyen JW, Crombez G, & Linton SJ (2016). The fear-avoidance model of pain. Pain, 157(8), 1588–1589. [PubMed: 27428892]

[11]. Balcombe J (2009). Animal pleasure and its moral significance. Applied animal behaviour science, 118(3–4), 208–216.

[12]. Kelley AE, & Berridge KC (2002). The neuroscience of natural rewards: relevance to addictive drugs. Journal of neuroscience, 22(9), 3306–3311. [PubMed: 11978804]

[13]. James DK (2010). Fetal learning: a critical review. Infant and Child Development: An International Journal of Research and Practice, 19(1), 45–54.

[14]. Samuni L, Mundry R, Terkel J, Zuberbühler K, & Hobaiter C (2014). Socially learned habituation to human observers in wild chimpanzees. Animal cognition, 17(4), 997–1005. [PubMed: 24500498]

[15]. Applewhite PB, Lapan EA, & Gardner FT (1969). Protozoan habituation learning after loss of macronuclei and cytoplasm. Nature, 222(5192), 491–492. [PubMed: 4976711]

[16]. Baluška F, & Levin M (2016). On having no head: cognition throughout biological systems. Frontiers in psychology, 7, 902. [PubMed: 27445884]

[17]. Thompson RF, & Spencer WA (1966). Habituation: a model phenomenon for the study of neuronal substrates of behavior. Psychological review, 73(1), 16. [PubMed: 5324565]

[18]. Bronstein PM, Neiman H, Wolkoff FD, & Levine MJ (1974). The development of habituation in the rat. Animal Learning & Behavior, 2(2), 92–96.

[19]. Castellucci V, Pinsker H, Kupfermann I, & Kandel ER (1970). Neuronal mechanisms of habituation and dishabituation of the gill-withdrawal reflex in Aplysia. Science, 167(3926), 1745–1748. [PubMed: 5416543]

[20]. Teyler TJ, & Alger BE (1976). Monosynaptic habituation in the vertebrate forebrain: the dentate gyrus examined in vitro. Brain Research, 115(3), 413–425. [PubMed: 974754]

[21]. Tang-Schomer MD, White JD, Tien LW, Schmitt LI, Valentin TM, Graziano DJ, Hopkins AM, Omenetto FG, Haydon PG, & Kaplan DL (2014). Bioengineered functional brain-like cortical tissue. Proceedings of the National Academy of Sciences, 111(38), 13811–13816.

[22]. Du C, Collins W, Cantley W, Sood D, & Kaplan DL (2017). Tutorials for electrophysiological recordings in neuronal tissue engineering. ACS Biomaterials Science & Engineering, 3(10), 2235–2246. [PubMed: 33445283]

[23]. Liaudanskaya V, Jgamadze D, Berk AN, Bischoff DJ, Gu BJ, Hawks-Mayer H, Whalen MJ, Chen HI, & Kaplan DL (2019). Engineering advanced neural tissue constructs to mitigate acute cerebral inflammation after brain transplantation in rats. Biomaterials, 192, 510–522. [PubMed: 30529870]

[24]. Chwalek K, Tang-Schomer MD, Omenetto FG, & Kaplan DL (2015). In vitro bioengineered model of cortical brain tissue. Nature protocols, 10(9), 1362. [PubMed: 26270395]

[25]. Valsamis B, & Schmid S (2011). Habituation and prepulse inhibition of acoustic startle in rodents. JoVE (Journal of Visualized Experiments), (55), e3446. [PubMed: 21912367]

[26]. Brennan PA, Hancock D, & Keverne EB (1992). The expression of the immediate-early genes c-fos, egr-1 and c-jun in the accessory olfactory bulb during the formation of an olfactory memory in mice. Neuroscience, 49(2), 277–284. [PubMed: 1279452]

[27]. Minatohara K, Akiyoshi M, & Okuno H (2016). Role of immediate-early genes in synaptic plasticity and neuronal ensembles underlying the memory trace. Frontiers in molecular neuroscience, 8, 78. [PubMed: 26778955]

[28]. Rayport SG, & Schacher S (1986). Synaptic plasticity in vitro: cell culture of identified Aplysia neurons mediating short-term habituation and sensitization. Journal of Neuroscience, 6(3), 759–763. [PubMed: 3958793]

[29]. Valsamis B, & Schmid S (2011). Habituation and prepulse inhibition of acoustic startle in rodents. JoVE (Journal of Visualized Experiments), (55), e3446. [PubMed: 21912367]

[30]. Wong K, Elegante M, Bartels B, Elkhayat S, Tien D, Roy S, … & Chung A (2010). Analyzing habituation responses to novelty in zebrafish (Danio rerio). Behavioural brain research, 208(2), 450–457. [PubMed: 20035794]

[31]. Lashley KS (1918). A simple maze: With data on the relation of the distribution of practice to the rate of learning. Psychobiology, 1(5), 353.

[32]. Gerbier E, & Toppino TC (2015). The effect of distributed practice: Neuroscience, cognition, and education. Trends in Neuroscience and Education, 4(3), 49–59.

[33]. Davis S, Bozon B, & Laroche S (2003). How necessary is the activation of the immediate early gene zif268 in synaptic plasticity and learning?. Behavioural brain research, 142(1–2), 17–30. [PubMed: 12798262]

[34]. Duclot F, & Kabbaj M (2017). The role of early growth response 1 (EGR1) in brain plasticity and neuropsychiatric disorders. Frontiers in behavioral neuroscience, 11, 35. [PubMed: 28321184]

[35]. Knapska E, & Kaczmarek L (2004). A gene for neuronal plasticity in the mammalian brain: Zif268/Egr-1/NGFI-A/Krox-24/TIS8/ZENK?. Progress in neurobiology, 74(4), 183–211. [PubMed: 15556287]

[36]. Li L, Yun SH, Keblesh J, Trommer BL, Xiong H, Radulovic J, & Tourtellotte WG (2007). Egr3, a synaptic activity regulated transcription factor that is essential for learning and memory. Molecular and Cellular Neuroscience, 35(1), 76–88. [PubMed: 17350282]

[37]. Poirier R, Cheval H, Mailhes C, Charnay P, Davis S, & Laroche S (2007). Paradoxical role of an Egr transcription factor family member, Egr2/Krox20, in learning and memory. Frontiers in behavioral neuroscience, 1, 6. [PubMed: 18958188]

[38]. Hadziselimovic F, Hadziselimovic NO, Demougin P, & Oakeley EJ (2014). Decreased expression of genes associated with memory and X-linked mental retardation in boys with non-syndromic cryptorchidism and high infertility risk. Molecular syndromology, 5(2), 76–80. [PubMed: 24715854]

[39]. Rouleau N, Cantley WL, Liaudanskaya V, Berk A, Du C, Rusk W, Peirent E, Koester C, Nieland TJF, & Kaplan DL (2020). A Long-Living Bioengineered Neural Tissue Platform to Study Neurodegeneration. Macromolecular Biosciences. 20(3), 1–8.

[40]. Dingle YTL, Liaudanskaya V, Finnegan LT, Berlind KC, Mizzoni C, Georgakoudi I, … & Kaplan DL (2020). Functional Characterization of Three-Dimensional Cortical Cultures for In Vitro Modeling of Brain Networks. IScience, 23(8), 101434. [PubMed: 32805649]

Higlights

- Non-associative learning responses were elicited in bioengineered neural tissues
- Upregulation of immediate early genes (IEG) were observed with distributed training
- Implications of studying fundamental features of cognition in vitro are discussed

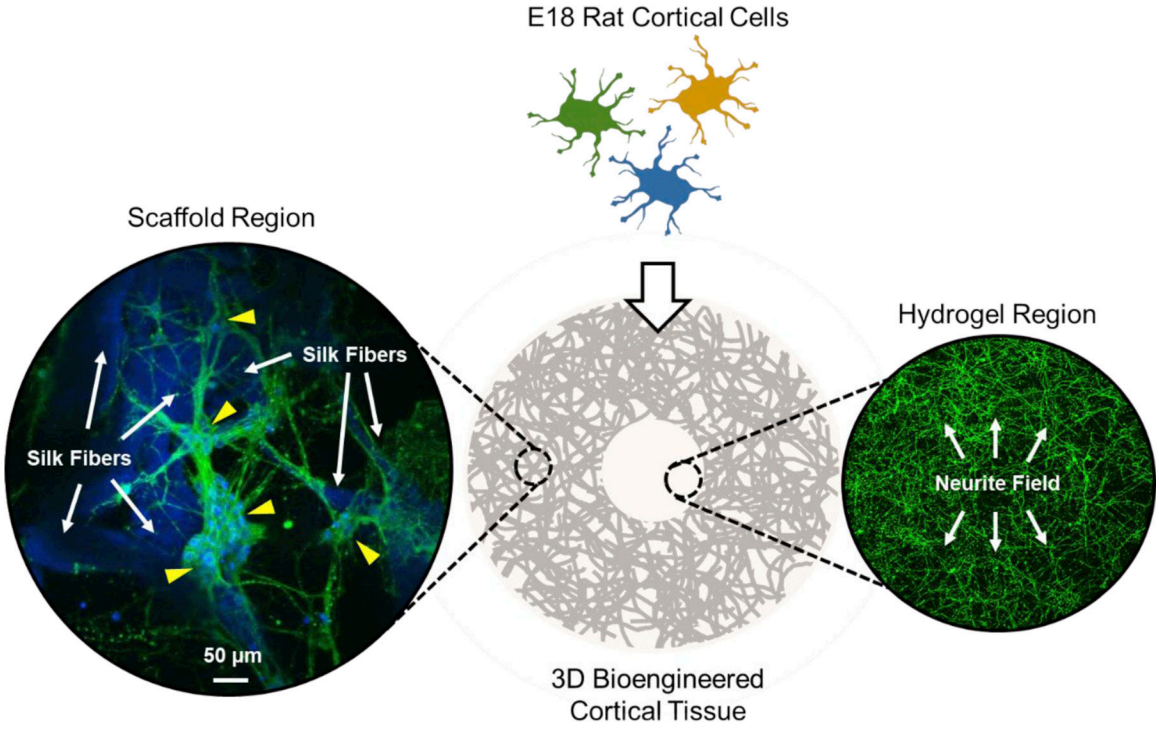

Figure 1. 3D bioengineered neural (cortical) tissues.

Rat cortical cells were isolated from embryonic pups (E18) and seeded in silk-based scaffolds to generate bioengineered cortical tissues. The scaffold region, rich with silk fibers (auto-fluorescent blue, indicated by white arrows), was densely populated by cell bodies (indicated by yellow arrows) and local neural networks whereas the hydrogel region of collagen was largely composed of a field of neurites, connecting distant regions of the tissue construct (green cell bodies = TUJ1, blue nuclei = DAPI).

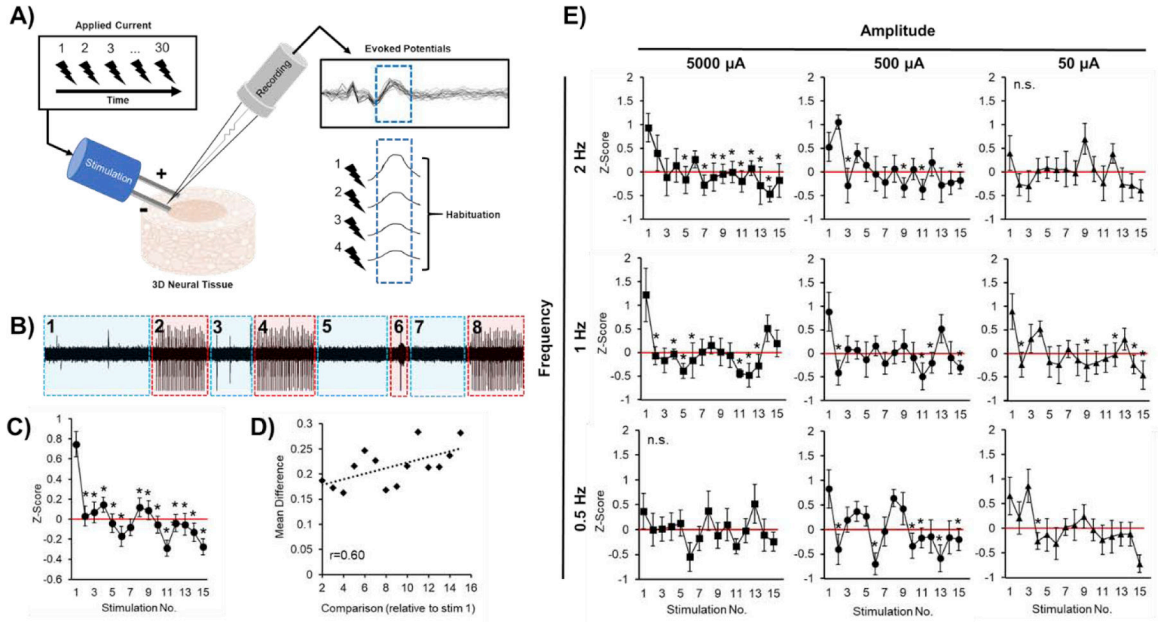

Figure 2. Bioengineered neural tissues display habituation responses.

Repetitive stimulation was applied to the surface of tissues while LFPs were collected, revealing EPs (A). Each trial began with a baseline period where spontaneous electrical activity could be observed (1) followed by 30 stimulations (2), a rest period with more spontaneous activity (3), a second set of 30 stimulations (4), another rest period (5), an injection of TTX marked by an artifactual spike upon perturbation of the extracellular medium (6), a final rest period during which TTX perfused (7), and a final 30 stimulations (8) (B). Examining an average of all trials (n=99), a significant decrement of EP magnitude was observed over the stimulation period (C) where mean differences between the first and each subsequent stimulation event increased over time, r=0.60 (D). Presented as individual groups, decrements were consistent across conditions of frequency and amplitude though with varying degrees of stability (E). Z-scores are normalized values that are not representative of EP magnitude in mV. Means ± SEMs are provided for each graph. Horizontal red lines indicate when z=0. Significant differences relative to the first EP are indicated, *p<0.05, n.s. = no significant difference (p>0.05).

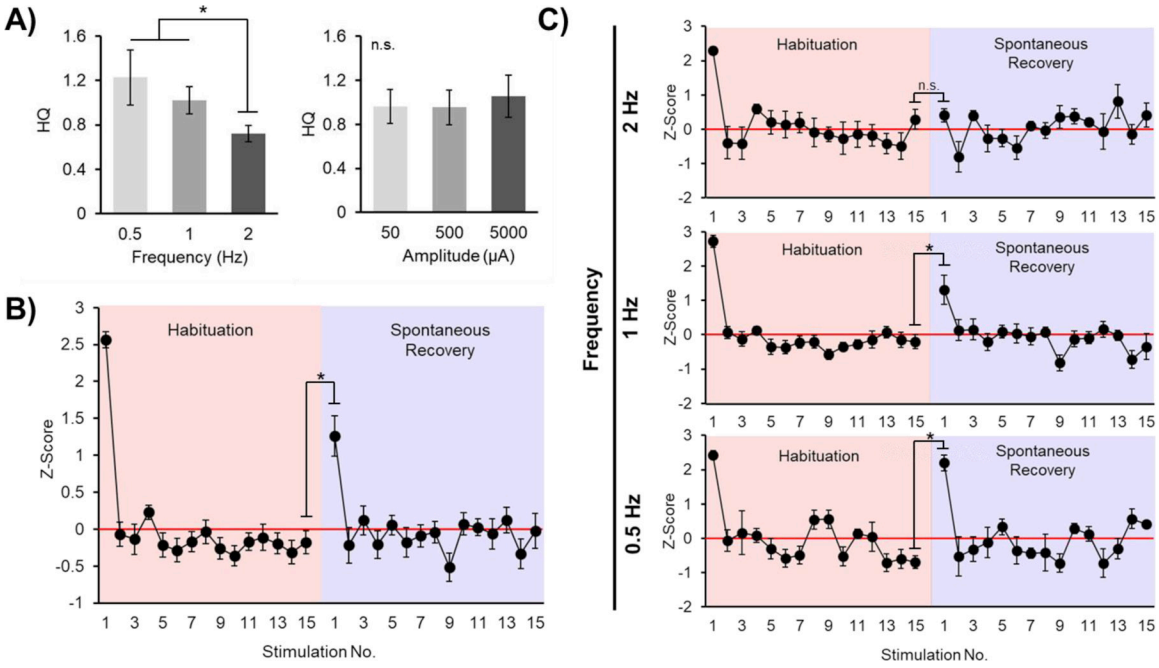

Figure 3. Habituation quotient (HQ) and spontaneous recovery are frequency-dependent.

HQ values were significantly diminished when exposed to 2 Hz stimuli relative to other conditions, indicating learning; there was no effect of current amplitude (A). Following the stimulation sequence (shaded red area) and a brief rest period, tissues were re-stimulated to test for the emergence of spontaneous recovery (shaded blue area). Examining a subset of trials (n=21) associated with habituation curves with an extreme initial (1st stimulation) normalized EP (z > 2), increased average normalized EP magnitude was observed during the spontaneous recovery phase followed by a secondary decrement of the response (B). Trials associated with the 2 Hz condition (n=5) did not display spontaneous recovery, while 1 Hz (n=12) and 0.5 Hz (n=4) conditions displayed increased normalized EP magnitude following the rest period (C). Means ± SEM are provided with significant differences indicated, *p<0.05, n.s. = no significant difference (p>0.05). Horizontal red lines indicate when z = 0.

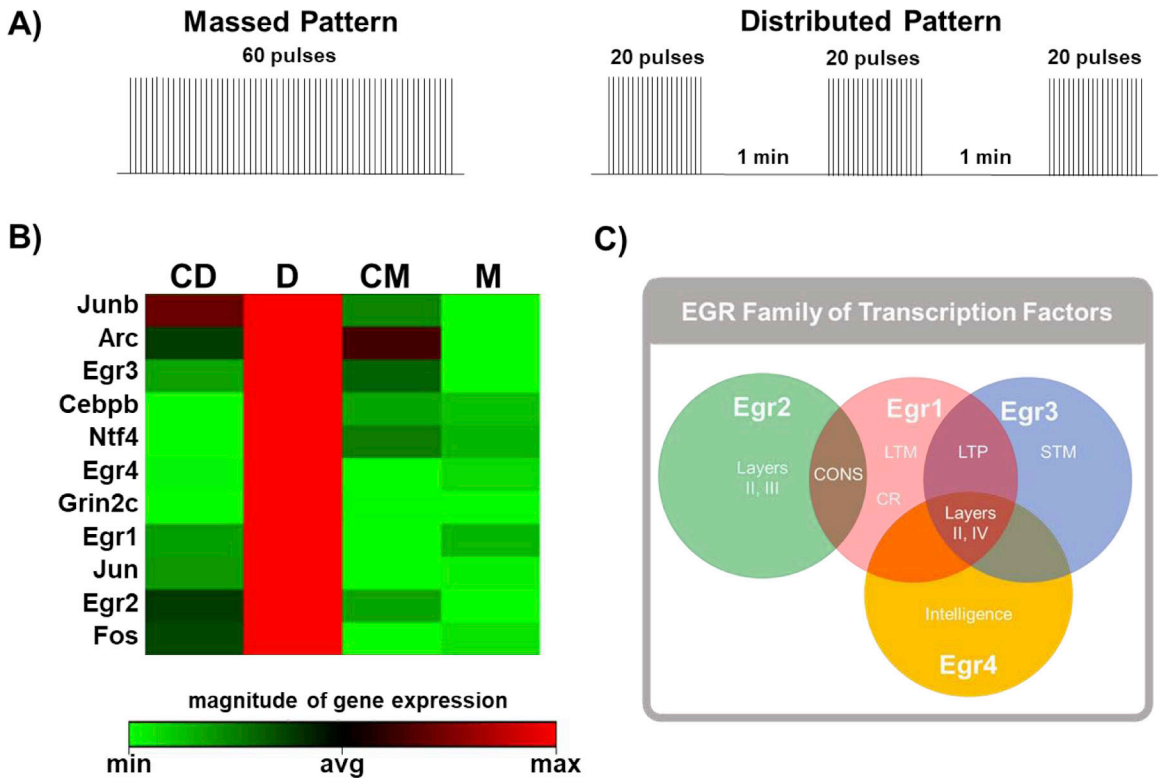

Figure 4. Genes in the early growth response (Egr) pathway are upregulated in response to distributed training.

Tissues were subjected to distributed (D), massed (M) or control stimulation protocols to assess synaptic plasticity (A). Samples were lysed to isolate RNA to determine relative expression levels using Qiagen RT² Profiler™ PCR Array for markers of Rat Synaptic Plasticity (catalog #ARN-126Z); red indicates maximal expression (B). Immediate early genes (IEGs) including Jun, Fos, and several members of the Egr family of genes emerged as collectively upregulated in samples exposed to distributed training. An overview of the EGR family of transcription-regulatory factors is provided including key characteristics and cortical layers of maximal expression (C). Labels: CONS = consolidation; LTM = long-term memory; CR = conditioned responses; LTP = long-term potentiation; STM = short-term memory.